Effect of Number and Position of Positive Charges on the Stacking of Porphyrins along Poly[d(A-T)(2)] at High Binding Densities

ARTICLE *in* THE JOURNAL OF PHYSICAL CHEMISTRY B · JUNE 2010

Impact Factor: 3.3 · DOI: 10.1021/jp1009687 · Source: PubMed

Effect of Number and Position of Positive Charges on the Stacking of Porphyrins along Poly[d(A-T)$_2$] at High Binding Densities

Jin-A Jung, Sang Hwa Lee, Biao Jin,† Youngku Sohn, and Seog K. Kim*

Department of Chemistry, Yeungnam University, Dae-dong, Gyeongsan City, Gyeong-buk, 712-749, Republic of Korea

Received: February 1, 2010; Revised Manuscript Received: March 25, 2010

At high porphyrin densities, the effects of the number and position of the positive charges of the periphery ring on the stacking of the porphyrin on poly[d(A-T)$_2$] was investigated using polarized spectroscopy, including circular and linear dichroism (CD and LD, respectively). The CD spectrum of *meso*-tetrakis(*N*-methylpyridinium-4-yl)porphyrin(TMPyP) consisted of two positive bands in the Soret absorption region at low [porphyrin]/[DNA base] ratios (*R* ratios) and changed to two distinguishable categories of the bisignate CD spectrum with increasing *R* ratio. These CD spectra were attributed to the monomeric groove binding, and the moderately and extensively stacked TMPyPs. In contrast, *trans*-bis(*N*-methylpyridinium-4-yl)porphyrin (*trans*-BMPyP) dominantly produced a CD spectrum that corresponded to the extensive stacking, except at the lowest *R* ratio that was used in this work ($R = 0.04$). However, for *cis*-bis(*N*-methylpyridinium-4-yl)porphyrin (*cis*-BMPyP), the intensity of the apparent bisignate CD signal was too small to assign it to the extensive stacking. Moreover, the shape of the CD spectrum in the DNA absorption region showed that the conformation of poly[d(A-T)$_2$] was retained, in contrast to the extensively stacked TMPyP and *trans*-BMPyP. In the extensively stacked TMPyP- poly[d(A-T)$_2$] assembly, the large negative LD signal in the Soret band was observed suggesting that the direction of the molecular planes of TMPyP was close to perpendicular with respect to the orientation axis (flow axis). In contrast, the LD spectrum of the *trans*-BMPyP-poly-[d(A-T)$_2$] complex produced positive LD signal in the same wavelength region, suggesting the orientation of the molecular plane was nearly parallel relative to the flow direction. Surprisingly, the LD signal in the DNA absorption region for both of the porphyrins was positive. Therefore, the helix axis of the DNA was near perpendicular relative to the flow direction in the porphyrin-polynucleotide assembly.

Introduction

Water-soluble cationic porphyrins bind to DNA, and since the pioneering work of Fiel[1−3] and Pasternack,[4] the interactions between these porphyrins and DNA have been the subject of intensive studies for potential applications in biological and medicinal sciences.[5−10] Several binding modes including intercalation between the DNA base-pairs,[11−13] groove binding,[13−20] outside binding,[21−23] and moderate and extensive stacking along the DNA template[23−32] have been exhibited for positively charged porphyrins and DNA. These various binding modes are affected by the nature and concentration of porphyrin, the ionic strength of the solution, and the sequence and conformation of the DNA. Additionally, the mixing order also affects the binding mode.[33] The nature of the DNA base is an essential factor for determining the binding mode of porphyrins. *Meso*-tetrakis(*N*-methylpyridinium-4-yl)porphyrin (hereafter referred to as TMPyP, Figure 1), a representative member of the porphyrin family, has been intercalated between the GC base-pairs of native DNA and poly[d(G-C)$_2$] at low [porphyrin]/[DNA] ratios (referred to as the *R* ratio), preferably at the 5′CG3′ site,[11,34] whereas it seems to binds across the minor groove of poly[d(A-T)$_2$].[35,36] As the porphyrin concentration increased, TMPyP started to stack along the DNA, poly[d(G-C)$_2$] and poly[d(A-T)$_2$]. For poly(dA)·poly(dT), the stacking occurred in the major groove.[30,31] The dependence of the stacking on the *R* ratio for TMPyP along poly[d(A-T)$_2$] and poly(dA)·poly(dT) has been well characterized. At intermediate *R* ratios, TMPyP "moderately" stacked along the AT bases, whereas the formation of the extensively stacked porphyrin assembly was apparent at higher ratios. Circular dichroism (CD) spectra are the best method of distinguishing between these two forms of stacking. For the moderate stacking, the CD in the Soret band is characterized by a bisignate spectrum with a positive band at a low energy level and a negative band at a short wavelength. The extensively stacked TMPyP also exhibits a bisignate CD spectrum but the order of the negative and positive bands are reversed, and the signal is more intense compared to the moderate stacking.

The position and number of the positive charges on the periphery rings of porphyrin also drastically affect the binding mode with respect to the DNA. When the cations of TMPyP are moved from the 4*N*- position to the 2*N*- position of the pyridinium ring, the rotation of the pyridinium ring is prohibited because of steric reasons, and porphyrin sits in the major groove of the native DNA, poly[d(A-T)$_2$] and poly[d(G-C)$_2$].[30,32,37,38] On the other hand, porphyrins with positive charges at the 4*N*- and 3*N*-positions of pyridinium ring intercalates between the base-pairs of the native DNA and poly[d(G-C)$_2$] at low binding ratios. Upon binding to poly[d(A-T)$_2$], the 4*N*-positively charged porphyrin (TMPyP) exhibited the monomeric and moderately stacking binding mode, whereas the 3*N*-positively charged porphyrin was extensively stacked along the poly[d(A-T)$_2$]

* To whom correspondence should be addressed. E mail: seogkim@yu.ac.kr. Tel: +82 53 810 2362. Fax: +82 53 815 5412.

† Present address: Instrumental Analysis Center, Yanbian University, Park Road 977, Yanji City, Jilin Province, 133002, China.

10.1021/jp1009687
Published on Web 05/13/2010

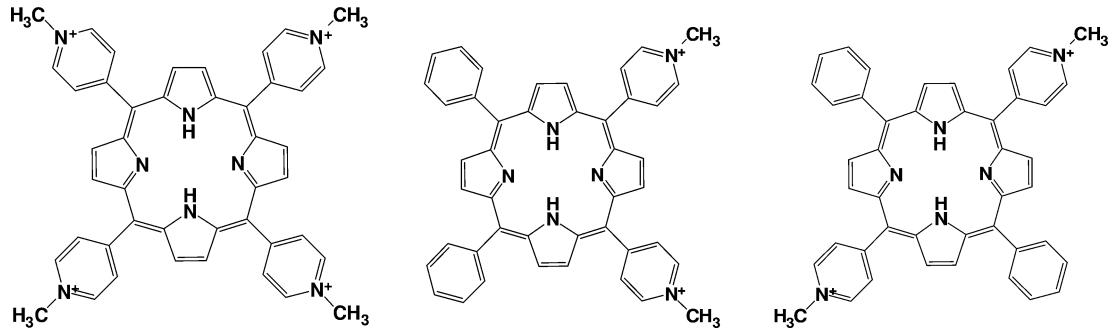

Figure 1. Chemical Structures of the TMPyP, *cis*-BMPyP, and *trans*-BMPyP porphyrins (from left).

template. The number of cations is also an important factor that governs the porphyrin binding mode to the DNA.[33,39−43] Neither *trans*- nor *cis*-bis(*N*-methylpyridinium-4-yl)porphyrin (referred to as *trans*- and *cis*-BMPyP, respectively, Figure 1), which contain two positive charges, intercalates between the base-pairs of the native DNA and poly[d(G-C)$_2$] even at the lowest R ratio.[43] Upon binding to poly[d(A-T)$_2$], both *trans*- and *cis*-BMPyP are stacked with characteristic bisignate CD spectra in the Soret absorption region at low R ratios (0.02−0.08). However, *trans*-BMPyP exhibited a groove binding mode at the lowest R ratio ($R = 0.02$).[43] The binding mode to DNA and poly[d(G-C)$_2$] were similarly stacked along the polynucleotide stem.

In this study, the effect of number and position of the positive charges on the stacking of porphyrins along poly[d(A-T)$_2$] was investigated at high binding densities using absorption measurements and CD and linear dichroism (LD) spectroscopy.

Experiments

Chemicals. The porphyrins were purchased from Frontier Scientific, Inc. (Utah, U.S.A.) and used without further purification. Poly[d(A-T)$_2$] was purchased from Amersham Biosciences (NJ, U.S.A.) and the other chemicals were purchased from Sigma-Aldrich. Poly[d(A-T)$_2$] was dissolved and purified according to a previously reported method.[43] A 5 mM cacodylate buffer was used throughout this work. The concentrations were spectrophotometrically measured using the following extinction coefficients: $\varepsilon_{421nm} = 2.45 \times 10^5$ cm^{-1} M^{-1}, $\varepsilon_{419nm} = 2.4 \times 10^5$ cm^{-1} M^{-1}, and $\varepsilon_{419nm} = 1.4 \times 10^5$ cm^{-1} M^{-1}, and $\varepsilon_{262nm} =$ 6600 cm^{-1} M^{-1} for TMPyP, *trans*-BMPyP, *cis*-BMPyP, and poly[d(A-T)$_2$] respectively. The concentration of poly[d(A-T)$_2$] was fixed at 50 μM in the base or phosphate, and the concentrations of the porphyrins were varied by adding aliquots of a concentrated porphyrin solution to poly[d(A-T)$_2$]. The appropriate volume corrections were made. The mixing ratio R, [porphyrin]/[DNA base], corresponded to the ratio of one porphyrin per polynucleotide bases, where $R = 0.01$ corresponded to one porphyrin per 100 DNA bases or phosphates. The spectral properties can be affected by the mixing order.[33] Therefore, the porphyrin was always added last, and the measurements were performed immediately after mixing.

Measurements. The absorption spectra were recorded on a Cary 100 Bio (Australia) spectrophotometer, and the CD spectra were recorded on a Jasco J810 (Tokyo, Japan) spectropolarimeter. The fluorescence emission spectra were recorded on a Jasco FP-777 spectrofluorimeter. The CD spectra was used to indicate the binding mode of porphyrin to DNA, particularly in the Soret absorption band, which was conceivably induced by the interaction between the two (B_x and B_y) electric transition moments of porphyrin and the chirally arranged DNA bases. The CD spectra of the porphyrin-polynucleotide mixture were averaged over the appropriate number of scans when it was necessary. The principles and the application of LD for the drug−DNA adduct system were well-described by Nordén and his co-workers.[44,45] The concept of LD spectra has been applied by Kim and his co-workers for the porphyrin-DNA complex system.[12,35,43] The measured LD spectra were divided by the absorption spectra in order to determine the dimensionless, wavelength-dependent quantity known as the reduced LD (referred to as LD^r), which is related to the angle, α, of the electric transition moment of the drug with respect to the local DNA helix axis through the following equation

$$LD^r = 1.5S(\langle 3\cos^2\alpha\rangle - 1)$$

In this equation, the orientation factor, S, can be determined by assuming the angle between the DNA base plane and the local helix axis is 86°. When the drug intercalates between the DNA base-pairs, the in-plane $\pi \rightarrow \pi^*$ transition of drug is parallel to the DNA base plane, and the LD^r magnitude in the drug absorption region should be similar to or larger than the DNA absorption region. A small magnitude or positive LD^r indicates that the drug's molecular plane is strongly tilted. In some porphyrin cases, the exact angle of the B_x and B_y electric transitions of the porphyrin relative to the DNA helix axis can be determined.[35,43]

Results

Absorption Spectrum. TMPyP has been known to bind at the minor groove of poly[d(A-T)$_2$] at extremely low R ratios and stack along the major groove as the porphyrin concentration increases.[15,18,19,30,37] Upon association with poly[d(A-T)$_2$], TMPyP exhibits a 9 nm red-shift from its absorption at 421 nm in the absence of poly[d(A-T)$_2$], and hypochromism was also observed in the Soret absorption region (Figure 2a) at low R ratios. The change in the absorption of the poly[d(A-T)$_2$] bound to TMPyP was small up to a mixing ratio of $R = 0.08$. From $0.08 < R < 0.20$, the absorbance decrease, and although it was not clear in the figure, an isosbestic point at 441 nm was observed in this mixing ratio range. Further increasing in the mixing ratio ($R > 0.20$) resulted in additional hypochromism and a blue shift in the Soret band. These absorptions indicated the presence of at least three poly[d(A-T)$_2$] bound TMPyP species with different absorption wavelength maxima and different extents of stacking. Figure 2(b) depicts the absorption spectrum of *cis*-BMPyP associated with poly[d(A-T)$_2$] in the Soret absorption region. A small, gradual decrease in the absorbance was observed with increasing mixing ratio, along with a small blue shift in maximum absorption to a shorter

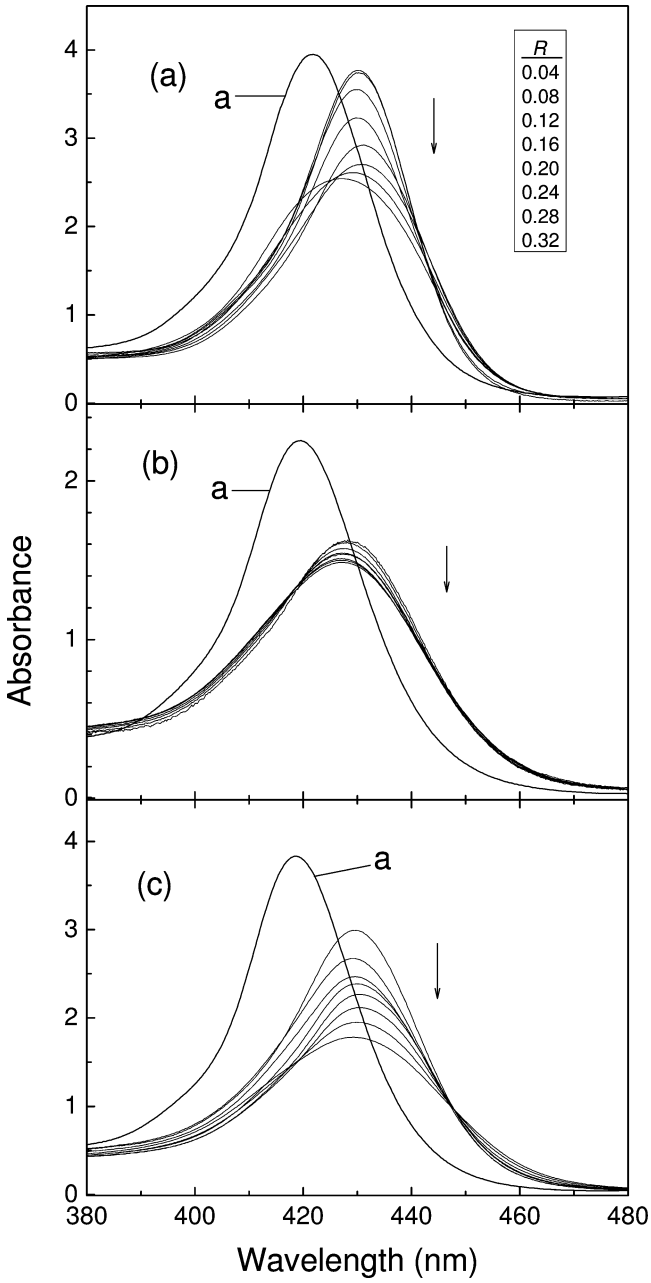

Figure 2. Absorption spectra of (a) TMPyP, (b) *cis*-BMPyP, and (c) *trans*-BMPyP. The [poly[d(A-T)$_2$] concentration was 50 μM in the DNA base, and the concentrations of porphyrin were 2−16 μM at increments of 2 μM. Thus, the mixing ratios, R = [porphyrin]/[DNA base], were 0.04, 0.08, 0.12, 0.16, 0.20, 0.24, 0.28, and 0.32. R increased in the direction of the arrows (insertion). All of the spectra were normalized to the highest porphyrin concentration. Curve a denotes the absorption spectrum of the DNA-free porphyrins that was recorded at a concentration of 4 μM and normalized to the highest concentration.

wavelength. At low R ratios, the change in absorption spectrum for *trans*-BMPyP was similar to *cis*-BMPyP (Figure 2c). However, further increasing the R ratio resulted in additional hypochromism and a small red-shift. The mixing ratio-dependent transition in the absorption spectrum of poly[d(A-T)$_2$] bound *trans*-BMPyP was accompanied by a clear isosbestic wavelength at 448 nm, suggesting that the transition occurred between the two bound species.

Circular Dichroism. The porphyrins that were investigated in this study are achiral and, hence, optically inactive. However, the association of these porphyrins with DNA and synthetic polynucleotide produced strong CD signals in the Soret absorption band because of the interaction of the electric transition of the porphyrins and the chirally arranged DNA bases. The CD spectra of TMPyP and *cis*-BMPyP bound to poly[d(A-T)$_2$] are depicted in Figure 3a,b, respectively. Upon association with poly[d(A-T)$_2$], TMPyP produced a CD spectrum that was complicatedly dependent on the R ratio (Figure 3(a)). At low mixing ratios ($R < 0.08$), the CD signal, which was represented by curve a in Figure 3a, was positive, and two positive maxima were observed at 421 and 439 nm, suggesting that the major binding mode at these low mixing ratios was groove binding. At intermediate R ratios ($0.08 < R < 0.16$), a negative minimum at 431 nm was observed. The positive maximum at the shorter wavelength shifted toward 418 nm, and the one at the longer wavelength shifted to 444 nm, confirming that TMPyP was moderately stacked. A typical CD spectrum of the TMPyP-poly[d(A-T)$_2$] complex is shown by curve b for R = 0.16 in Figure 3a. Further increasing the TMPyP concentration ($R > 0.20$) resulted in a bisignate CD spectrum (curve c in Figure 3a) with a negative minimum at 433 nm and a positive maximum at 446 nm, suggesting that TMPyP was extensively stacked. The shape and intensities of the bisignate CD spectra at $R > 0.20$ were identical. The apparent bisignate CD spectra at high mixing ratios agreed with previously reported results.[15,18,19,30,37] In contrast, *cis*-BMPyP produced a bisignate but very weak CD signal upon binding to poly[d(A-T)$_2$]. At the lowest *cis*-BMPyP concentration, the CD spectrum was too weak to record. At R = 0.08, the bisignate CD spectrum consisted of a negative minimum at 422 nm and a positive maximum at 441 nm. As the R ratio increased, the magnitude of the CD spectra increased, even though they were normalized with

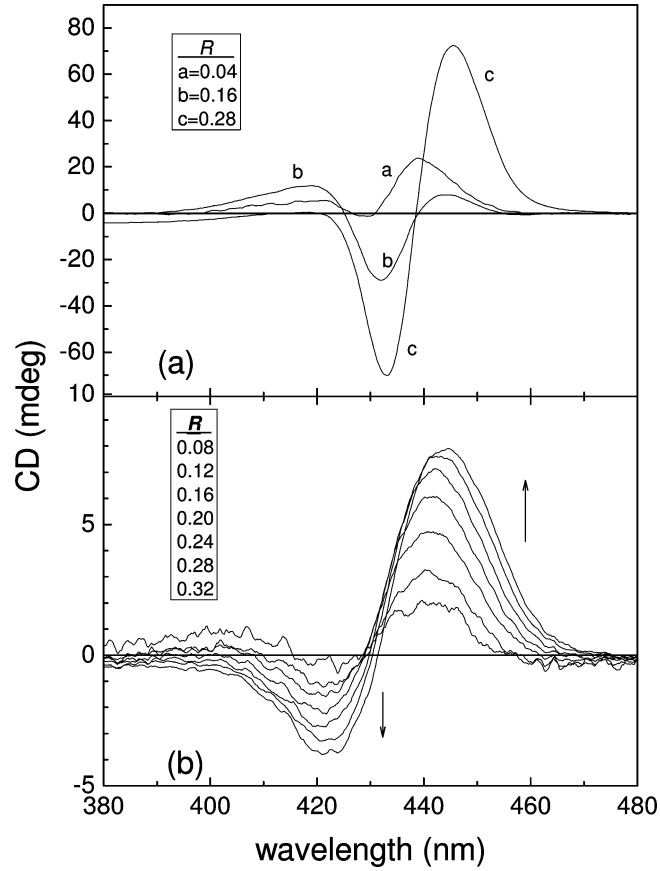

Figure 3. Representative CD spectra of the (a) TMPyP-poly[d(A-T)$_2$] and (b) *cis*-BMPyP-poly[d(A-T)$_2$] complexes. The mixing ratios for the spectra that were marked as a, b, and c are shown into (a). In (b), the R ratio is shown and increased in direction of the arrows. The concentration of poly[d(A-T)$_2$] was 50 μM in the DNA base.

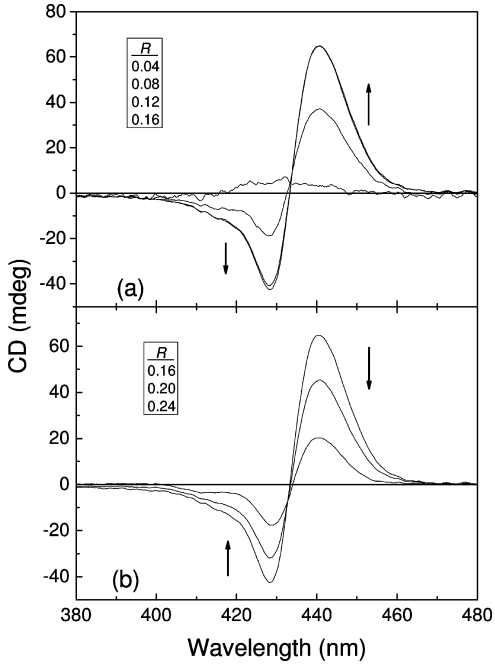

Figure 4. CD spectrum of the *trans*-BMPyP-poly[d(A-T)$_2$] complex. The *R* ratio increased in the direction of the arrows. The concentration of poly[d(A-T)$_2$] was 50 μM in the DNA base.

the highest concentration. Additionally, the positive maximum shifted to 444 nm, whereas the negative minimum remained at 422 nm. At the highest mixing ratio, the CD intensity was almost one tenth of the TMPyP-poly[d(A-T)$_2$] complex.

Figure 4 depicts the CD spectra of the *trans*-BMPyP-poly[d(A-T)$_2$] complex. At the lowest *R* ratio that was tested in this work, $R = 0.04$, the CD spectrum was positive in the entire Soret absorption region with a maximum at 434 nm, suggesting that *trans*-BMPyP exhibited a groove binding mode.[43] However, at $R = 0.08$, a bisignate CD spectrum was observed, and the shape resembled the extensively stacked TMPyP-poly[d(A-T)$_2$] complex, with an apparent negative minimum at 428 nm and a positive maximum at 441 nm. Both the maximum and minimum wavelengths were shifted to short wavelengths by ~5 nm compared to the TMPyP case. Spectra observed at $R = 0.12$ and 0.16 were identical and shapes were similar to the spectrum at $R = 0.08$. However, the intensities of these two spectra were larger than the spectrum at $R = 0.08$. Further increasing the *R* ratio decreased the CD intensity without changing the shape, which is in contrast with TMPyP case. Moreover, no evidence in CD spectrum for the presence of moderately stacked species was observed in the *trans*-BMPyP case.

In general, the discussion in the CD spectra of the porphyrin-DNA complexes in DNA absorption region is ambiguous because the origin of the change in the CD spectra is not clear. The change in the CD spectra in the DNA absorption region originated from either the change in the DNA conformation after the porphyrin binding or the accumulation of the induced CD of the porphyrin-DNA complex. However, the CD spectra were drastically dependent on the nature of the porphyrins in the DNA absorption region in Figure 5. In the absence of porphyrin, poly[d(A-T)$_2$] exhibited a CD spectrum that consisted of a negative minimum at 248 nm, a positive band at 265 nm, and a shoulder near 277 nm, which corresponded to the B form of poly[d(A-T)$_2$]. After the addition of TMPyP, the magnitude of the negative band at the short wavelength decreased and eventually became positive, whereas the positive CD band at the long wavelength became a large negative signal. At a high

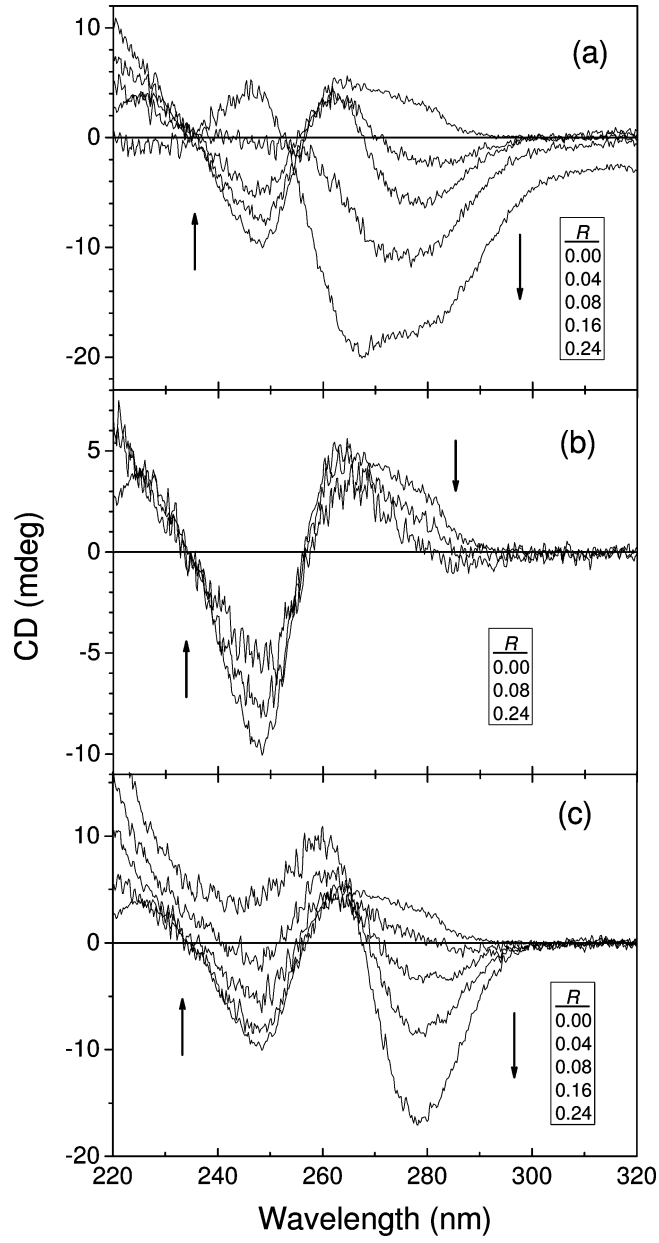

Figure 5. Selective CD spectra of the (a) TMPyP-, (b) *cis*-BMPyP-, and (c) *trans*-BMPyP-poly[d(A-T)$_2$] complexes in the DNA absorption region. The *R* ratio increased in the direction of the arrows. The concentrations were the same as in Figures 4 and 5. In the DNA absorption region, the shapes of the CD spectra were identical for $R =$ 0.20, 0.24, 0.28, and 0.32 for all of the porphyrins and therefore, only the spectra for $R = 0.24$ were shown.

TMPyP concentration ($R = 0.24$), the CD spectrum of the TMPyP-poly[d(A-T)$_2$] complex was characterized by a positive band at 246 nm, a negative minimum at 268 nm, and a shoulder near 282 nm. On the other hand, the *cis*-BMPyP binding did not significantly alter the shape of the CD spectra even at the highest concentration ($R = 0.24$), but the overall intensity somewhat decreased. The change in the spectra for *trans*-BMPyP was similar to TMPyP, where the negative minimum became positive, and the positive band became negative. However, the shape of the apparent CD spectrum at $R = 0.24$ for the *trans*-BMPyP-poly[d(A-T)$_2$] complex somewhat deviated from the TMPyP complex,: with a positive maximum located at 259 nm and a negative minimum at 279 nm. The *trans*-BMPyP-poly[d(A-T)$_2$] complex did not exhibit a should in contrast to TMPyP.

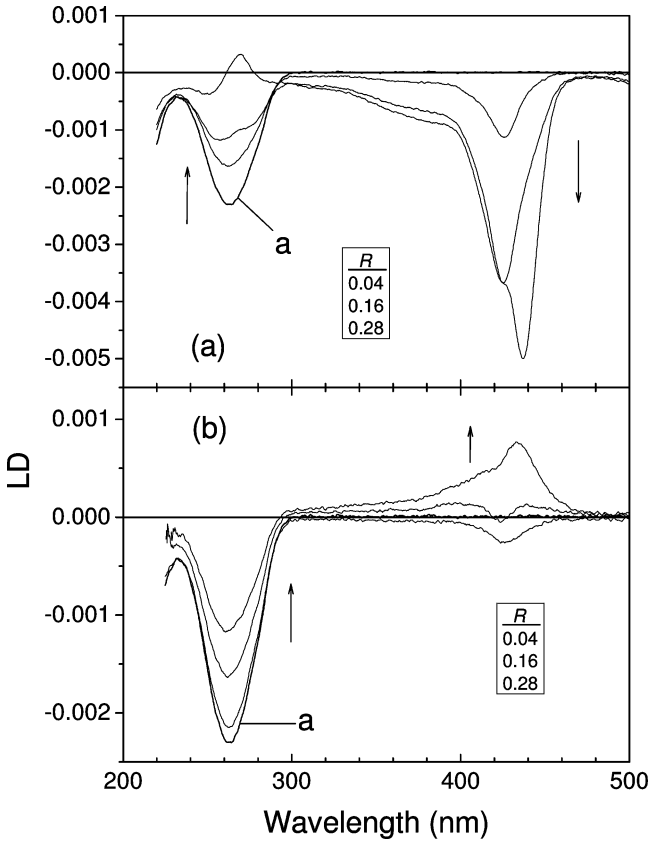

Figure 6. Selective LD spectra of the (a) TMPyP-poly[d(A-T)$_2$] and (b) *cis*-BMPyP-poly[d(A-T)$_2$] complexes. The mixing ratios are shown and increased in the direction of the arrows. The concentration of poly[d(A-T)$_2$] was 50 μM in the DNA base.

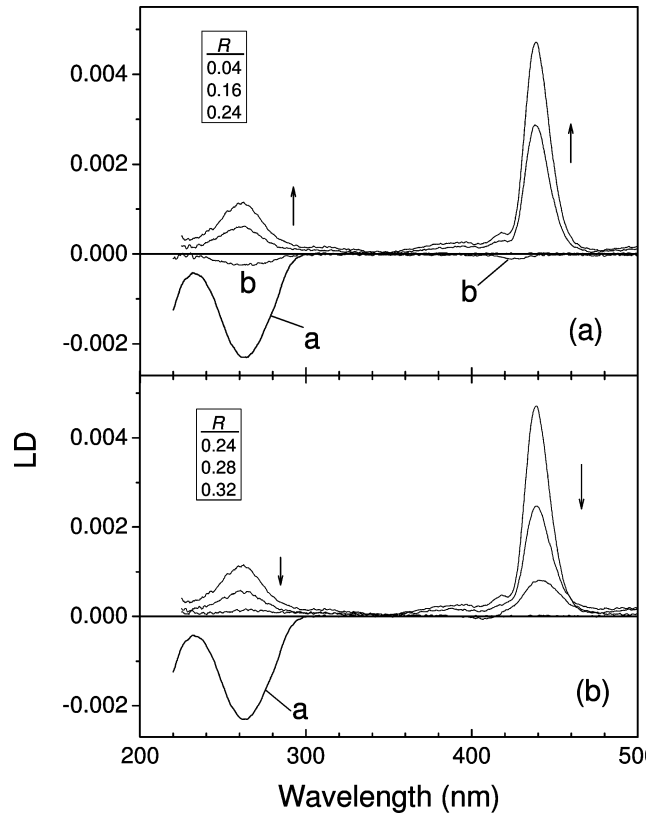

Figure 7. Selective LD spectra of the *trans*-BMPyP-poly[d(A-T)$_2$] complex at (a) low and (b) high *R* ratios. The concentration of poly[d(A-T)$_2$] was 50 μM in the DNA base. Curve a represents the LD spectrum of the porphyrin-free poly[d(A-T)$_2$]. The LD spectrum of the *trans*-BMPyP-poly[d(A-T)$_2$] complex at the lowest *R* ratio was denoted by b in panel (a).

LD and LD^r. The LD spectra of the porphyrin-poly[d(A-T)$_2$] complexes also exhibited a drastic dependence on the nature of the porphyrins. The LD spectrum of poly[d(A-T)$_2$] produced a negative LD signal in the DNA absorption region with the expected shape resemble from the LD set up that was adopted in this study.[44,45] In Figure 6a, the binding of TMPyP decreased the magnitude of the negative LD signal in the DNA absorption region and increased the signal in the Soret region for the selected mixing ratios. The decrease in the negative LD signal in the DNA absorption region was possibly caused by either the decreased orientation ability of the DNA as the result of the TMPyP binding or the positive contribution from DNA-bound TMPyP, or both. The latter reason may not be ignored in this case because the positive LD signal was apparent in the DNA absorption region at the highest mixing ratio. In the Soret absorption region, TMPyP produced a negative LD band at all of the mixing ratios. However, as the *R* ratio increased, the negative band shifted from 426 to 425 nm, corresponding to the transition from the monomeric binding to the moderate stacking. This minimum shifted to 437 nm as the TMPyP extensively stacked. The band at the low *R* ratios was retained in the form of a shoulder at higher mixing ratios, suggesting the presence of the moderately stacked species even at a high *R* ratios. Figure 6b shows the LD spectrum of the *cis*-BMPyP-poly[d(A-T)$_2$] complex at a few selective *R* ratios. As the *R* ratio increased, the magnitude of the LD signal in the DNA absorption region decreased but not as much as for TMPyP. The shape of LD was retained in this region. However, in the Soret region the change was drastic, and the negative signal became positive despite the small change in the absorption and CD spectra. Therefore, the binding geometry of stacked *cis*-BMPyP changed, whereas the conformation of the DNA did not change much. The most drastic alteration in the LD spectrum was observed for *trans*-BMPyP. Although very small negative signals in both the DNA absorption region and the Soret region were observed at low *R* ratios, the LD signal was almost entirely diminished at a *R* ratio of 0.08 (Figure 7a). Further increasing the mixing ratio resulted in positive LD signals in both the DNA absorption region and the Soret region with the maxima at 261 and 438 nm, respectively. The intensity of the positive signals reached a maximum at a *R* ratio of 0.24. This peculiar positive LD in both the DNA and the porphyrin absorption regions suggested that the DNA helix axis and the axis normal to the stacked porphyrin molecular plane were nearly perpendicular with respect to the flow direction. Further increasing the *R* ratio resulted in a collapse in the LD signal (Figure 7b), which was also accompanied by a collapse in the CD signal, suggesting the aggregation of the *trans*-BMPyP-poly[d(A-T)$_2$] complex. A similar positive LD signal has been reported for *meso*-tetrakis(*N*-methylpyridium-3-yl)porphyrin, where the position of the cation moved from the 4*N*- to 3*N*-pyridiumyl ring position, which was equivalent to moving the N^+-CH_3 cation from the *para*- to the *meta*- position with respect to the *meso*-carbon.[32] However, in that work, the CD spectrum in the DNA absorption region was retained in contrast to the inversed CD spectrum that was observed for the *trans*-BMPyP complex in this study.

The magnitude of the LD^r in the DNA absorption region mainly reflected the orientation ability of polynucleotide. In Figure 8a,b for TMPyP and cis-BMPyP, respectively, the magnitude of the negative LD^r gradually decreased with increasing porphyrin loading, suggesting a bent or partial

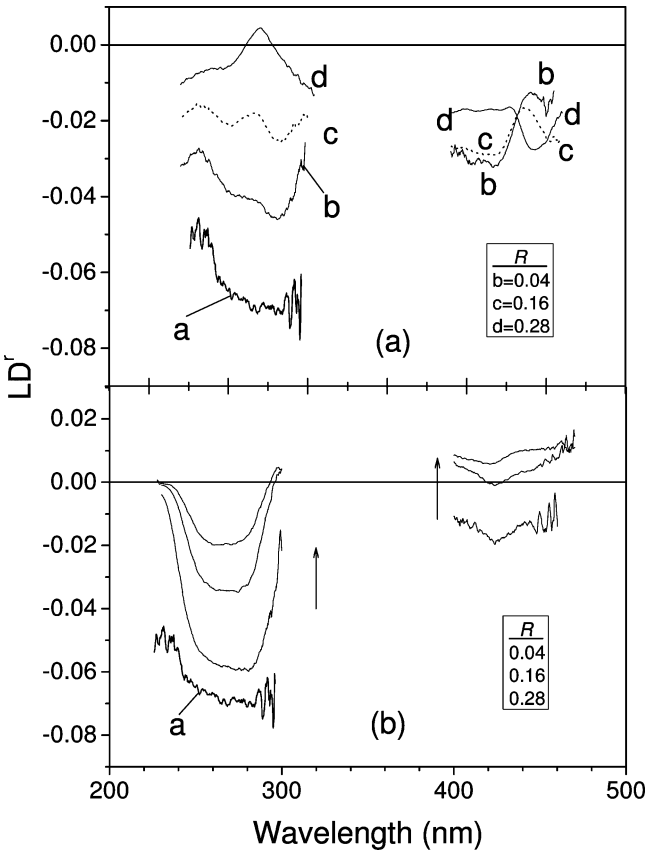

Figure 8. Representative LD^r spectra of the (a) TMPyP- and (b) *cis*-BMPyP-poly[d(A-T)$_2$] complexes at a few selected R ratios. The porphyrin-free poly[d(A-T)$_2$] spectra is denoted by a in both graphs. The TMPyP-poly[d(A-T)$_2$] spectra at $R = 0.16$ is denoted by the dotted curve and is also marked as c. The symbols b and d in panel (a) denote R ratios of 0.04 and 0.28, respectively.

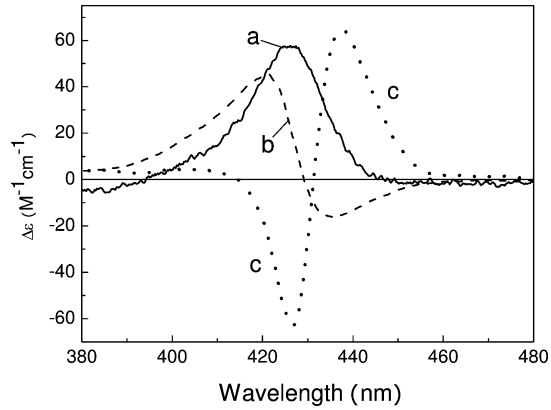

Figure 9. Typical CD spectra for monomeric (curve a), moderately stacked (curve b), and extensively stacked (curve c) TMPyP. Curves b and c are the CD spectra of TMPyP-d[(A-T)$_{12}$]$_2$ at [TMPyP]/[oligonucleotide] ratios of 0.4 and 2.0, respectively. See text.

dissociation of the polynucleotide stem near the porphyrin binding site. For TMPyP, the positive contribution from the bound porphyrin was also clearly visible, particularly at the high R ratios. Therefore, the angle of the B_x and B_y transitions in the Soret absorption band, which corresponded to the angle of the molecular plane of the porphyrin with respect to the local DNA helix axis, can be calculated from the LD^r values for the monomerically bound porphyrins, where absorption and LD spectra are the sums of the contributions from the two transitions.[12,35] However, when the porphyrins were stacked, which is the case for both TMPyP and *cis*-BMPyP in this current study, the absorption and the LD signal in the Soret band reflected the sum of the transition of the electric transition vectors. Therefore, the individual transition moment was not separable. Furthermore, the exact orientation factor, S, could be calculated for the drug-free DNA assuming the average angle between the DNA base plane and the local helix was of 86°, but this calculation could not be made because the contribution from porphyrins affected the LD^r value in the DNA absorption region at high R ratios. Nevertheless, the angles that were calculated from the current LD^r spectra could provide some insight into the difference in the binding modes between TMPyP and *cis*-BMPyP. The angles, α, that were calculated from the maximum and minimum values of the LD^r in the Soret region for the TMPyP-poly[d(A-T)$_2$] complex at $R = 0.04$ were 75 and 61°, respectively, which were in the same range as the angles of 68−78° and 61−63° that were obtained from the low R ratios.[43] Although the LD^r spectrum of the TMPyP-poly[d(A-T)$_2$] complex was similar in the Soret region at $R = 0.16$, the positive contribution from the bound porphyrin was too large to calculate the angles for this complex. At higher mixing ratios, the LD^r was positive in the DNA absorption region and the shape was reversed in the Soret absorption region. For *cis*-BMPyP (Figure 8b), the calculated angles were 62 and 59° at $R = 0.04$ and 49 and 45° at $R = 0.28$. The former angles were similar to 54−62° and 51−55°, which were obtained from the low mixing ratios.[43] The latter values coincided with the drug being bound at the minor groove of the DNA, even though this was not likely the case for the *cis*-BMPyP-poly[d(A-T)$_2$] complex. The *trans*-BMPyP-poly[d(A-T)$_2$] complex produced a positive LD signal in the DNA absorption region, resulting in a positive LD^r value, which in turn, prevented the calculation of the orientation factor at this current stage. Therefore, this case was not shown in this work.

Discussion

Extensive and Moderate Stacking of Porphyrins along poly[d(A-T)$_2$]. The observed CD spectra, especially for TMPyP and *trans*-BMPyP, corresponded to the combination of the monomerically bound, and moderately and extensively stacked porphyrins. The shape of the CD spectrum that were measured for the TMPyP-d[(A-T)$_{12}$]$_2$ complex at a [TMPyP]/[oligonucleotide] ratio = 0.4, or $R = 0.017$ corresponded to monomerically bound TMPyP, whereas the spectra at a [TMPyP]/[oligonucleotide] ratio = 2.2 or $R = 0.094$ corresponded to the moderated stacked TMPyP. Additionally, the shape of the CD spectrum for the extensively stacked TMPyP was obtained by subtracting the properly adjusted monomer and moderately stacked CD spectrum from the measured CD spectrum of the TMPyP-poly[d(A-T)$_2$] complex at high R ratios. This method assumed that the CD spectrum that represented the extensively stacked TMPyP was antisymmetric, that is, the intensity of the positive and negative CD bands were identical.[31] The CD spectrum that was obtained from this treatment is depicted in Figure 9. On the basis of this representative CD spectrum, the CD spectrum of the TMPyP-poly[d(A-T)$_2$] at the lowest mixing ratio (R = 0.04) mainly consisted of the monomerically bound TMPyP. Then the CD spectrum corresponded to the combination of a positive CD band that was caused by the monomerically bound TMPyP and the presence of a negative band from the moderately and/or extensively stacked TMPyP rather than the presence of two positive bands. At intermediate mixing ratios, for example at $R = 0.16$, the positive contribution near 418 nm was larger than the monomeric CD despite a negative or zero contribution

from the extensively stacked TMPyP, and the positive contribution near 444 nm was smaller than the monomeric CD. Therefore, a non-negligible amount of the moderately stacked species was present. In summary, the monomerically bound, moderately stacked, and extensively stacked TMPyP were sequentially the main binding modes for the TMPyP-poly[d(A-T)$_2$] complex as the relative porphyrin concentration increased. In other words, even at the extreme *R* ratios that were adopted in this study, the possibility of the presence of the other binding modes could not completely be ruled out.

In contrast, although it was small, a pure positive CD band that was observed at the $R = 0.04$ for the *trans*-BMPyP-poly[d(A-T)$_2$] complex strongly suggested that the dominating species in this condition was the monomerically bound porphyrin. One of the large differences in the binding modes between TMPyP and *trans*-BMPyP was that the relative amount of the moderately stacked species was very small in the *trans*-BMPyP case although positive contribution near 425 nm. which might have been caused by the traces of the positive band of the moderately stacked porphyrin at the short wavelength, were observed at all of the mixing ratios. Another difference was the saturation *R* ratio. For TMPyP, The CD spectrum that corresponded to extensive stacking appeared at $R > 0.20$, whereas the saturated mixing ratio for *trans*-BMPyP was 0.12, and the extensively stacked species dominated even at the lower mixing ratios. Finally, for *trans*-BMPyP, the CD spectra of the extensively stacked species decreased with increasing mixing ratio, suggesting the aggregation of the *trans*-BMPyP-poly[d(A-T)$_2$] complex. These observed differences suggested that the presence of two cations at the *trans*-position was essential whereas, the two additional positive charges of TMPyP inhibited the formation of the extensive stacked porphyrin assembly.

At a glance, the shape of the CD spectra of the *cis*-BMPyP-poly[d(A-T)$_2$] complex in the Soret band was similar to the extensively stacked TMPyP or *trans*-BMPyP. However, essential differences were observed. The intensity was very low and was about one-tenth of the extensively stacked TMPyP and *trans*-BMPyP. Second, the band widths of both the positive and negative CD signals were far wider for *cis*-BMPyP compared to the extensively stacked TMPyP and *trans*-BMPyP. Moreover, the conformation of the CD spectrum did change much in the DNA absorption (see below). All of these observations suggested that the *cis*-BMPyP complex ineffectively stacked along the poly[d(A-T)$_2$] stem if stacking occurred at all. Another possible binding mode, where the two electric transition moments of the porphyrin interacted with the chirally arranged DNA base in the opposite direction resulting in a bisignate CD spectrum, could not completely be ruled out for *cis*-BMPyP. If the porphyrins stacked and interact strongly with each other along poly[d(A-T)$_2$] stem, the conformation of the bound polynucleotide was conceivably expected to be largely distorted, which was not the case for *cis*-BMPyP.

The large bisignate CD in the Soret absorption region that represented the extensively stacked porphyrin was accompanied by a negative CD signal near 280 nm in the DNA absorption region for the *trans*-BMPyP complex. On the other hand, this signal was positive in the absence of porphyrin. An additional negative band was observed near 270 nm and was significant for TMPyP. Therefore, this negative CD band probably corresponded to the moderately stacked species. These negative contributions of the CD spectrum in the DNA absorption region resembled the CD spectrum of Z-form DNA. However, an extreme ionic concentration is required for the formation of the Z-form DNA for AT sequences. Therefore, the negative CD spectrum may be originated from porphyrin although the absorbance of porphyrin was very weak in this wavelength region.

Binding Modes of Porphyrins. Both the LD and LD^r magnitudes of poly[d(A-T)$_2$] in DNA absorption region decreased upon the binding of TMPyP or *cis*-BMPyP, suggesting that some of the orientation ability was lost, in general, because of the bending or the increased flexibility of the polynucleotide. For instance, binding positively charged metal ions to the negatively charged phosphate group of the DNA through electrostatic attraction decreased the repulsive interaction between the phosphate groups, which in turn increased the flexibility of the DNA. However, this was not observed for the porphyrins. For *cis*-BMPyP, the shape of the LD and LD^r spectra as well as the CD spectrum were retained in the DNA absorption region in spite of the heavy porphyrin loading. Therefore, the conformation of poly[d(A-T)$_2$] was not significantly altered by the binding of *cis*-BMPyP. Rejecting the possibility of the conformation change, the decrease in the LD magnitude was caused by the bending of the polynucleotide stem, where the DNA bent after the binding of *cis*-BMPyP. The accumulation of *cis*-BMPyP along the DNA stem resulted in additional bending of the polynucleotide stem, causing the DNA helix axis to tilt. This effect could have the caused the *R* ratio-dependent change in the angle of the B_x and B_y transitions with respect to the local DNA helix axis. However, for TMPyP, a positive contribution was observed with increasing *R* ratio, even though the LD and LD^r signals in the Soret absorption region were negative. In the complex formed with poly[d(A-T)$_2$], the B_x and B_y electric transition moment tilt with difference extent with respect to the local DNA hemix axis.

At high *R* ratios, stacked assemblies formed for both the TMPyP and *trans*-BMPyP-DNA complexes with poly[d(A-T)$_2$]. The shape of the assembly was asymmetric, allowing the complexes to orient in the flow. In other words, the difference in the length of the long and short axes of the assembly was large enough to be oriented in the flow, resulting in a significant LD signal. In the *trans*-TMPyP assembly, the directions of both the polynucleotide helix axis and the porphyrin stacking axis that was normal to the molecular plane of porphyrin were nearly perpendicular rather than parallel with respect to the flow axis (orientation axis), as was evident from the positive LD spectra in both the DNA absorption region and the Soret band. In contrast, the direction of the polynucleotide helix axis for TMPyP was nearly perpendicular, whereas the porphyrin's stacking axis was close to parallel relative to the flow axis. These results were confirmed from the positive contribution in the LD spectrum for the DNA absorption region and the large negative LD signal in the Soret region. Finally the main contribution to the flow orientation for both *trans*-BMPyP and TMPyP was the porphyrin assembly rather than the DNA because, even when the LD signal was near zero for some mixing ratios, large positive or negative LD signals were observed for *trans*-BMPyP and TMPyP, respectively. These results differed from other drug−DNA systems, where the appearance of the LD signal in the flow was usually assigned to the orientation of the DNA stem.

Conclusion

TMPyP exhibited a gradual change in the binding mode upon binding to poly[d(A-T)$_2$] from a monomeric groove binding, and moderate stacking to extensive stacking as the *R* ratio increased. The binding mode was mixed even at extremely low or high *R* ratios. On the other hand, *trans*-BMPyP produced a

CD spectrum that was almost entirely attributed to the extensive stacking although the monomeric groove binding mode was observed at the lowest *R* ratio. However, the CD intensity of *cis*-BMPyP was too low to be assigned to the extensively stacked porphyrin. The different interactions of the B_x and B_y transitions with the DNA bases was not completely ruled out as the reason for the bisignate CD of *cis*-BMPyP. These results indicated that two positive charges were required at the *trans*-position for the extensive stacking. The two additional positive charges that originated from pyridium inhibited the formation of the extensive stacking.

Acknowledgment. This study was supported by the National Research Foundation of Korea (Grant 2009 0083855).

References and Notes

(1) Fiel, R. J.; Howard, J. C.; Datta-Gupta, N. *Nucleic Acid Res.* **1979**, *6*, 3093–3118.
(2) Fiel, R. J.; Datta-Gupta, N.; Mark, E. H.; Howard, J. C. *Cancer Res.* **1981**, *41*, 3543–3545.
(3) Fiel, R. J.; Beerman, T. A.; Mark, E. H.; Datta-Gupta, N. *Biochem. Biophys. Res. Commun.* **1982**, *107*, 1067–1074.
(4) Pasternack, R. F.; Gibbs, E. J.; Villafranca, J. J. *Biochemistry* **1983**, *22*, 2406–2414.
(5) Granville, D. J.; McManus, B. M.; Hunt, D. W. *Histol. Histopathol.* **2001**, *16*, 309–317.
(6) Vicente, M. G. *Curr. Med. Chem.: Anti-Cancer Agents* **2001**, *1*, 175–194.
(7) Ding, L.; Balzarini, D.; Schols, D.; Meunier, B.; Clercq, E. *Biochem. Pharmacol.* **1992**, *44*, 1675–1679.
(8) Guang, L.; Yuan, F.; Xi, M.; Zhao, C.; Liu, L.; Wen, E.; Ai, Y. *China Med. J.* **2003**, *116*, 1248–1252.
(9) Nicotera, T. M.; Munson, B. R.; Fiel, R. J. *Photochem. Photobiol.* **1994**, *60*, 295–300.
(10) Onuki, J.; Ribas, A. V.; Medeiros, M. H.; Araki, K.; Toma, H. E.; Catalani, L. H.; DiMascio, P. *Photochem. Photobiol.* **1996**, *63*, 272–277.
(11) Guliaev, A. B.; Leontis, N. B. *Biochemistry* **1999**, *38*, 15425–15437.
(12) Lee, Y.-A.; Lee, S.; Cho, T.-S.; Kim, C.; Han, S. W.; Kim, S. K. *J. Phys. Chem. B* **2002**, *106*, 11351–11355.
(13) Strickland, J. A.; Marzilli, L. G.; Wilson, W. D. *Biopolymers* **1990**, *29*, 1307–1323.
(14) Strickland, J. A.; Marzilli, L. G.; Wilson, W. D. *Biopolymers* **1990**, *29*, 1307–1323.
(15) Kuroda, R.; Tanaka, H. *J. Chem. Soc., Chem. Commun.* **1994**, *157*, 5–1576.
(16) Schneider, H.-J.; Wang, M. *J. Org. Chem.* **1994**, *59*, 7473–7478.
(17) Pasternack, R. F.; Goldsmith, J. I.; Gibbs, E. J. *Biophys. J.* **1998**, *75*, 1024–1031.
(18) Yun, B. H.; Jeon, S. H.; Cho, T.-S.; Yi, S. Y.; Sehlstedt, U.; Kim, S. K. *Biophys. Chem.* **1998**, *70*, 1–10.
(19) Lee, S.; Jeon, S. H.; Kim, B.-J.; Han, S. W.; Jang, H. G.; Kim, S. K. *Biophys. Chem.* **2001**, *92*, 35–45.
(20) Park, T.; Kim, J. M.; Han, S. W.; Lee, D.-J.; Kim, S. K. *Biochim. Biophys. Acta* **2005**, *1726*, 287–292.
(21) Carvlin, M. J.; Datta-Gupta, N.; Fiel, R. J. *Biochem. Biophys. Res. Commun.* **1982**, *108*, 66–73.
(22) Carvlin, M. J.; Fiel, R. J. *Nucleic Acids Res.* **1983**, *11*, 6121–6139.
(23) Banville, D. L.; Marzilli, J. A.; Strickland, J. A.; Wilson, W. D. *Biopolymers* **1986**, *25*, 1837–1858.
(24) Mukundan, N. E.; Pethö, G.; Dixon, D. W.; Marzilli, L. G. *Inorg. Chem.* **1995**, *34*, 3677–3687.
(25) Mallamace, F.; Micali, N.; Monsu'Scolaro, L.; Pasternack, R. F.; Romeo, A.; Terracina, A.; Trusso, S. J. *J. Mol. Struct.* **1996**, *383*, 255–260.
(26) Pasternack, R. F.; Gibbs, E. J.; Collings, P. J.; dePaula, J. C.; Turzo, L. C.; Terracina, A. *J. Am. Chem. Soc.* **1998**, *120*, 5873–5878.
(27) Pasternack, R. F.; Gibbs, E. J.; Bruzewicz, D.; Stewart, D.; Engstrom, K. S. *J. Am. Chem. Soc.* **2002**, *124*, 3533–3539.
(28) Pasternack, R. F. *Chirality* **2003**, *15*, 329–332.
(29) Scolaro, L. M.; Romeo, A.; Pasternack, R. *J. Am. Chem. Soc.* **2004**, *126*, 7178–7179.
(30) Lee, Y.-A.; Kim, J.-O.; Cho, T.-S.; Song, R.; Kim, S. K. *J. Am. Chem. Soc.* **2003**, *125*, 8106–8107.
(31) Kim, J.-O.; Lee, Y.-A.; Yun, B. H.; Han, S. W.; Kwaq, S. T.; Kim, S. K. *Biophys. J.* **2004**, *86*, 1012–1017.
(32) Park, T.; Shin, J. S.; Han, S. W.; Son, J.-K.; Kim, S. K. *J. Phys. Chem. B.* **2004**, *108*, 17106–17111.
(33) Ismail, M.; Rodger, P. M.; Rodger, A. *J. Biomol. Struct. Dyn.* **2000**, *11*, 335–348.
(34) Ford, K.; Neidle, S. *Bioorg. Med. Chem.* **1995**, *6*, 671–677.
(35) Jin, B.; Lee, H. M.; Lee, Y.-A.; Ko, J. H.; Kim, C.; Kim, S. K. *J. Am. Chem. Soc.* **2005**, *127*, 2417–2424.
(36) Chae, Y.-H.; Jin, B.; Kim, J.-K.; Han, S. W.; Kim, S. K.; Lee, H. M. *Bull. Korean Chem. Soc.* **2007**, *28*, 2203–2208.
(37) Lee, S.; Lee, Y.-A.; Lee, H. M.; Lee, J. Y.; Kim, D. H.; Kim, S. K. *Biophys. J.* **2002**, *83*, 371–381.
(38) Lee, Y.-A.; Lee, S.; Lee, H. M.; Lee, C.-S.; Kim, S. K. *J. Biochem.* **2003**, *133*, 343–349.
(39) Pasternack, R. F.; Giannetto, A.; Pagano, P.; Gibbs, E. J. *J. Am. Chem. Soc.* **1991**, *113*, 7799–7800.
(40) Pasternack, R. F.; Bustamante, C.; Collings, P. J.; Giannetto, A.; Gibbs, E. J. *J. Am. Chem. Soc.* **1993**, *115*, 5393–5399.
(41) Sari, M. A.; Battioni, J. P.; Dupre, D.; Mansuy, D.; Le Pecq, J. B. *Biochem. Pharmacol.* **1988**, *37*, 1861–1862.
(42) Gibbs, E. J.; Tinoco, I., Jr.; Maestre, M. F.; Ellinas, P. A.; Pasternack, R. F. *Biochem. Biophys. Res. Commun.* **1988**, *157*, 350–358.
(43) Jin, B.; Ahn, J. E.; Ko, J. H.; Wang, W.; Han, S. W.; Kim, S. K. *J. Phys. Chem. B* **2008**, *112*, 15875–15882.
(44) Rodger, A.; Nordén, B. *Circular Dichroism and Linear Dichroism*; Oxford University Press: New York, 1997.
(45) Eriksson, M.; Nordén, B. *Methods Enzymol* **2001**, *340*, 68–98.

JP1009687